2015 IEEE/RSJ International Conference on Intelligent Robots and Systems (IROS)
Congress Center Hamburg
Sept 28 - Oct 2, 2015. Hamburg, Germany

A Spider-Inspired Dragline Enables Aerial Pitch Righting in a Mobile Robot

Stacey Shield†, Callen Fisher† *Student Member, IEEE* and Amir Patel†, *Student Member, IEEE*

***Abstract* – This paper presents a novel approach to achieving aerial pitch righting in a mobile robot, inspired by the draglines used by jumping spiders. We developed and simulated a mathematical model of the spider during the aerial phase of its jump to gain further insight into the factors affecting the pitch response. The results demonstrate that the dragline could also potentially function as a brake, slowing the spider down before landing. Subsequently, we developed a small robotic platform to demonstrate dragline-based aerial pitch righting on a robot experimentally. Lastly, the possible size and weight advantages over other pitch righting methods are discussed.**

I. Introduction

While mobile robots excel when operating under controlled conditions such as those in a laboratory or factory, their ability to manoeuvre effectively in natural environments lags far behind that of animals. One of the challenges when navigating rough or arboreal terrain is the occurrence of ballistic phases, either intentionally through jumping or unintentionally as in falls [1]. In order to prevent damage, robots and animals alike must be able to reorient themselves in the air such that they land in a favourable position.

Terrestrial animals, lacking dedicated structures for aerial control, often achieve this by zero-angular-momentum methods including back twisting, most associated with cats [1][2], or the rapid rotation of a tail exhibited by many reptiles [1][3][4][5]. Robots inspired by cats [2] and lizards [3][4][5] have demonstrated that these methods are not only effective when applied to robots, but actually compare favourably to traditional alternatives such as reaction wheels [3]. The disadvantage of angular-momentum-based righting is that the structures involved need to be either large, massive or fast-moving relative to the body to be effective [6].

A possible alternative to these methods, which does not have this limitation, was the focus of a recent study by Chen et al. [7] into pitch righting in the salticid family of jumping spiders. Before leaving the substrate, these spiders attach a silk dragline [7]. They then apply tension to this line while in the air, using an internal friction brake [8], creating a moment that can be used to control the pitch [7]. In experiments reported in [7], salticid spiders jumping with an initial backward rotation were able to reverse this motion and land in a safe position with their bodies approximately parallel to the ground. Spiders of similar size and structure jumping without the line continued to rotate backwards throughout the jump, landing at a much steeper body angle and often bouncing or somersaulting before coming to rest. This can be seen in Fig. 1, which shows a comparison between spiders jumping with and without the dragline.

Although the aforementioned study was the first to examine pitch righting in salticids specifically, previous researchers have hypothesized that the dragline could be used for this purpose. In the first study into the mechanism of jumping in these spiders, Parry and Brown [9] observed that, when a spider's dragline broke mid-air, the animal was unable to reverse its initial backward pitch and flipped over completely. A later study by Hill [10] reiterated their conclusions regarding the importance of the dragline in aerial control. It has also been postulated that the dragline is used to control pitch in jumps by the wandering spider [11], which is significant as these spiders are much larger than salticid species and tend to pitch forward initially rather than backward. Aside from these studies, there has been almost no research into the mechanisms of jumping or aerial control in spiders.

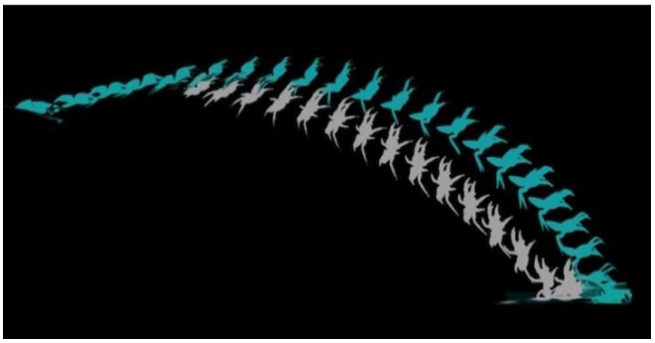

Fig. 1: Comparison between spiders jumping with (blue) and without silk (grey.) It can be seen that, with the dragline, the spider was able to reorient itself such that it landed at a shallow body angle. Image source: Yung-Kang Chen [7].

The purpose of this paper is to investigate whether the dragline can be adapted for pitch righting in a mobile robot. In Section II, a mathematical model is developed for the body and dragline system. Restricting the system to planar motion controlled by a single degree-of-freedom (DOF) line under constant tension, this model is used to determine the effects of initial velocity and silk force magnitude on the pitch response of the spider. Section III addresses the design of a simple robotic platform, and its use in experiments to validate the performance of the mathematical model. Section IV presents the results of these experiments with discussion and conclusions. The ability of the dragline to alter the pitch of a robot, its characteristics as a control system and its performance compared to other established methods of aerial control are emphasised.

Corresponding author: shlsta001@myuct.ac.za
†Department of Electrical Engineering, University of Cape Town, South Africa

II. Modelling and Analysis

A. Assumptions and Generalized Coordinates

The spider and dragline system was modelled in planar motion. Although small relative motions between the cephalothorax, abdomen and legs do occur during the jump [7], it was assumed that their effects on the moment of inertia of the body are negligible, and hence the spider is modelled as a single rigid body. The shape of the spider was approximated as a sphere with its diameter equal to the animal's body length, l.

As the line must be pulled taut to exert a force on the body, it was modelled as a rigid, massless rod. The line was connected at a distance r from the body's centre of mass (CoM) producing a system similar to a double pendulum, but with the length L of the first pendulum being variable.

This system can be described by three generalized coordinates: L, θ_0 – the angle of the line anticlockwise from the substrate, and θ_S – the angle of the line anticlockwise from the body axis. The coordinates of interest are taken to be the position (x, z) of the CoM in the inertial frame, and the pitch angle θ_A of the abdomen anticlockwise from the positive x axis. The relationship between these coordinate systems is given in (1) to (3). The complete model is illustrated in Fig. 2.

$$x = L\cos(\theta_0) - r\cos(\theta_0 - \theta_S) \quad (1)$$

$$z = L\sin(\theta_0) - r\sin(\theta_0 - \theta_S) \quad (2)$$

$$\theta_A = \theta_0 - \theta_S \quad (3)$$

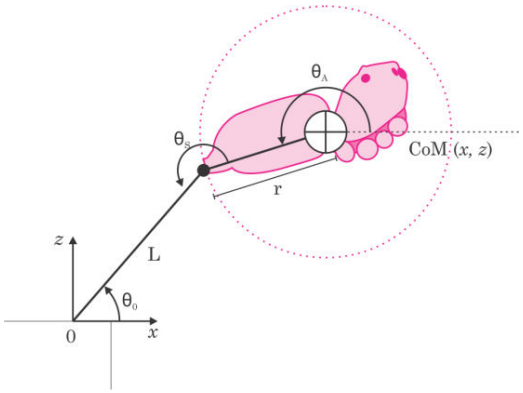

Fig. 2: The mathematical model of the dragline and spider.

Based on the average size of the salticids studied by Chen, *et al*. [7], the mass and length of the body were set to 19.95 mg and 6.1 mm respectively.

B. Equations of Motion

While in the air, three forces act on the spider: gravity, the silk force F_s and aerodynamic drag F_D [7]. The drag force was estimated using the equation:

$$F_D = \frac{1}{2} C_d \rho A v^2 \quad (4)$$

where v is the magnitude of the CoM velocity, A is the projection area facing the direction of motion, ρ is the air density (taken as 1 kg m^{-3} as in [7]) and C_d is the coefficient of drag. $C_d$was set as 1.5, as Chen *et al*. [7] found that this value best predicted the instantaneous velocity of the spider at each point in their study.

The magnitude of the silk force F_s is the control input. It is mapped to a generalized force opposing the coordinate L. Although tension in the line was found to decrease towards the end of the jump in the spiders observed [7], to simplify analysis a constant F_s is used initially.

Using the Lagrange-Euler method [12][13], the system dynamics were modelled in the form of the general manipulator equation:

$$\boldsymbol{M}(\boldsymbol{q})\ddot{\boldsymbol{q}} + \boldsymbol{C}(\boldsymbol{q}, \dot{\boldsymbol{q}})\dot{\boldsymbol{q}} + \boldsymbol{G}(\boldsymbol{q}) = \boldsymbol{B}(\boldsymbol{q})F_S \quad (5)$$

with the generalized coordinate vector $\boldsymbol{q} = [\theta_0 \quad \theta_s \quad L]^T$. The matrices $\boldsymbol{M}$, $\boldsymbol{C}$, $\boldsymbol{G}$ and $\boldsymbol{B}$ have been omitted in the interest of brevity and because they are fairly trivial to derive.

C. Simulation

The model was simulated using MATLAB/Simulink. To validate the accuracy of the model, the plot of approximate silk force from Chen, *et al*. [7] was digitized and used as an input to the simulation. A comparison between the abdomen angle response from the original paper and the simulated response is shown in Fig. 3. Aside from an offset in each axis, it can be seen that the forms of the responses are similar.

The following factors could account for the discrepancies between the model and the observed jump:

- The mass, length and initial velocity of the spider performing this particular jump were not provided, so an the average for all the sample salticids was used [7].
- The moment of inertia of the spider was not stated [7], so we approximated it as a rectangular box of size $l \times 0.5l \times 0.5l$.
- Our approximation of the drag forces did not account for changes in the projected area caused by small changes in the animal's posture.

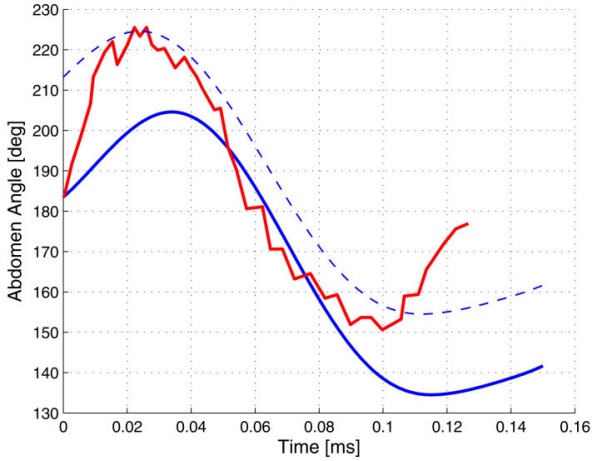

Fig. 3: Comparison between the simulated θ_A response (blue) and the observed response [7] (red). The dashed line removes the offset in the simulated response for clearer comparison.

To allow the model to be assessed visually, it was also animated using V-Realm virtual reality software. Fig. 4 compares this animation to a salticid jump recorded in [7].

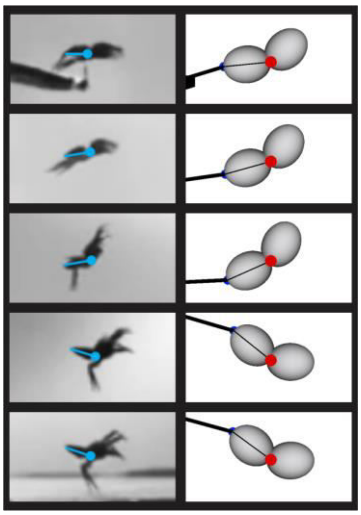

Fig. 4: Comparison between video stills of the salticid (left) and an animation of the model (right). Image source: Yung-Kang Chen [7]

Having validated the model, two tests were performed, one varying the magnitude of the silk force F_s and the other varying the initial velocity v_0, with the launch angle θ_i and the initial angular velocity ω_{Ai} held constant. The simulation was terminated when the CoM reached a position 3.5 cm* below the starting point as this represented the ground height. A third test, where the stopping condition was removed and the simulation allowed to run for 10 seconds, was used to generate a phase portrait of the system. The parameter values used for each test are listed in Table 1. Note that F_s is measured in terms of body weight (BW) as in [7].

TABLE 1 SIMULATION PARAMETERS†

	F_s [BW]	v_0 [m s^{-1}]	θ_i [deg]	ω_{Ai} [deg s^{-1}]
Test 1	0.05:0.05:1	0.99	11.4	661
Test 2	0.26	0.25:0.25:2	11.4	661
Test 3	0.26	0.99	11.4	661

Based on these simulations, it was found that, for constant F_s the pitch angle response (in radians) takes on the form of a sinusoid oscillating about a decaying exponential. This is approximated by the equation:

$$\theta_A(t) = C_1 \cos\left(\frac{2\pi t}{\tau_1} - \varphi\right) + C_2\, e^{\frac{-t}{\tau_2}} + \frac{\pi}{2} \qquad (6)$$

where C_1, C_2, τ_1, τ_2 and φ are constants determined by the parameters examined.

As can be seen from (6), as time increases, the angle will tend towards a position of oscillation about 90°. This is supported by analysis of the phase portrait (see Fig. 5) which shows vertices about the point corresponding to a pitch of 90° and zero angular velocity, indicating a limit cycle at this point. The phase portrait also indicates that the system is unstable when at rest at an abdomen angle of 270°, as this corresponds to a saddle point. Physically, this indicates that the spider may oscillate about a position where it hangs vertically with its abdomen up, but the same position with its abdomen down is unstable.

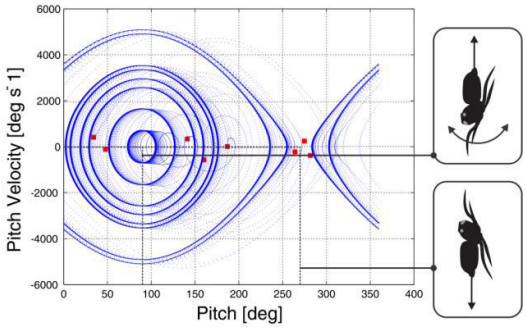

Fig. 5: Phase portrait for the spider model showing vertices and a saddle point about the points where the system is at rest at abdomen angles of 90° and 270° respectively. The red markers indicate the start of each trajectory.

The θ_A responses for varying F_s and v_0 are compared in Fig. 6. The angle, as well as the time at which the first pitch reversal occurred tended to increase with v_0 and decrease with F_s, as shown in Fig. 7. Despite this, increasing either F_s or v_0 would tend to cause the pitch to reverse more often in the jump, as increasing initial velocity also increased the time in the air.

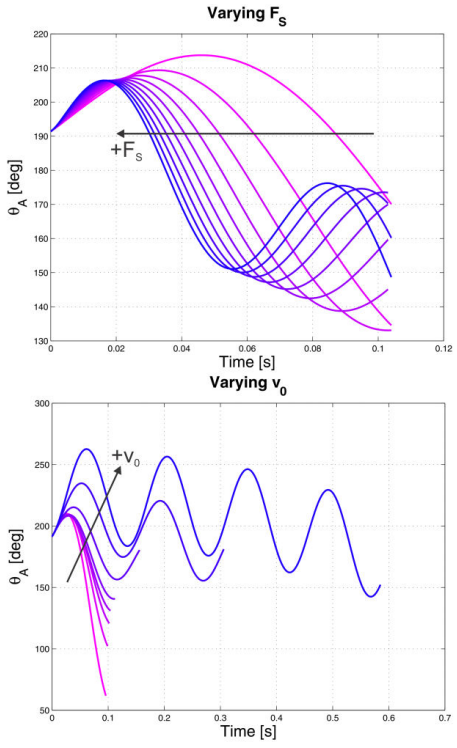

Fig. 6: θ_A responses for varying F_0 and v_0. It can be seen that increasing either quantity will cause pitch to reverse more often during the jump.

* This was the difference in elevation between the starting point and the endpoint in [7]

† The fixed values of F_s, v_0 and θ_i were taken to be their averages for the salticid jumps in [7]. The fixed value of ω_{Ai} was obtained using the average $\Delta\theta_A$ and air time for the non-silk spiders in [7].

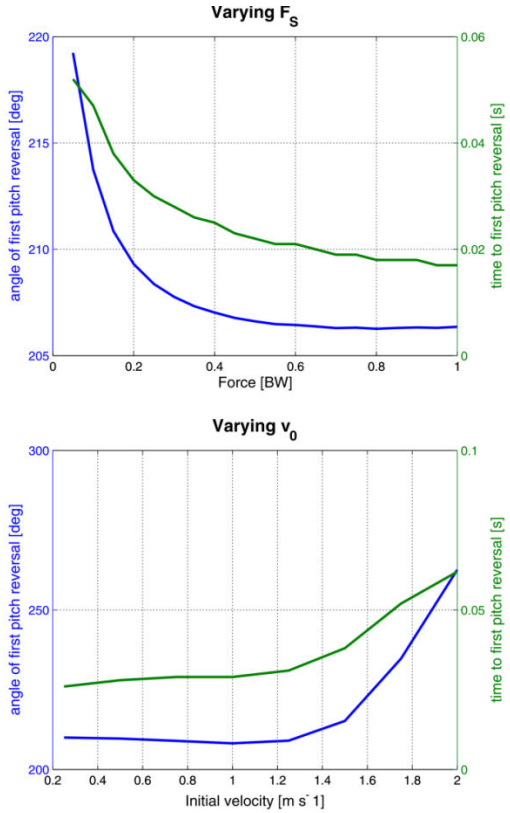

Fig. 7: The angle and time of initial pitch reversal for varying F_s and v_0 is depicted above.

Besides the effects on the pitch response, it was also noted that the final horizontal velocity decreased with increasing F_s. This was also observed to occur in salticids, where the dragline is hypothesized to act as not only a pitch stabilizer but also a brake to slow the animal down [7]. A plot of the final horizontal velocity at different magnitudes of silk force is given in Fig. 8.

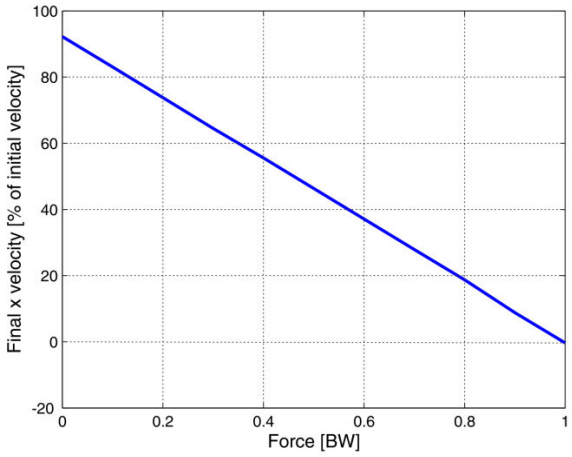

Fig. 8: Plot of the final x velocity at different magnitudes of silk force. The reduction in velocity is greater when more force is applied.

III. Robotic Platform

A. *Robot Design*

To confirm the ability of the dragline to bring about pitch righting in practice, a Line-Equipped Autonomous Platform (LEAP) was designed. This was propelled into the air by a simple catapult-like launcher, as illustrated in Fig. 9.

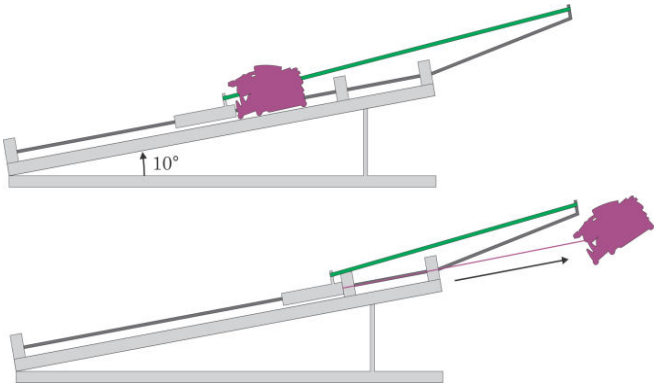

Fig. 9: Illustration showing the action of the launcher.

To minimize the force necessary to launch the robot, the first design requirement was that it be small and light. It would also have to be durable to withstand the impact of landing. To satisfy these criteria, the LEAP's chassis was constructed using the construction toy, LEGO Technic™. Besides being made from strong, lightweight plastic, these parts allow for rapid construction, modification and repairs to the design.

Braided fishing line was used for the dragline as it is intended to withstand large tensile forces, but it would not retain the shape of the spool as in nylon fishing line. To enable active control of the tension in the dragline, the spool was directly coupled to a 7 mm diameter coreless DC motor such that the motor would oppose the unreeling of the line when switched on.

An ST iNEMO-M1 inertial module was used to control the motor as well as track the motion of the LEAP. This device is equipped with a three-axis digital accelerometer (LSM303DLHC) and three-axis digital gyroscope (LSGD20), allowing it to detect both the linear and angular motion of the robot. This data was transmitted wirelessly to the base station computer using XBEE-PRO® radio frequency modules. Samples were taken at a frequency of 100 Hz. Additionally, two GoPro HERO3 Black Edition cameras were used to record the motion of the robot at 240 fps: one was placed perpendicular to the plane of the jump, and the other behind the robot such that unwanted yaw or roll could be easily detected. LEDs were fitted to the nose and tail of the robot so its position could be clearly identified in videos. The electronics on the robot were powered by a 7.4 V lithium ion battery.

Photographs of the complete LEAP are shown in Fig. 10. With all components and electronics the robot weighs a total of 88 g.

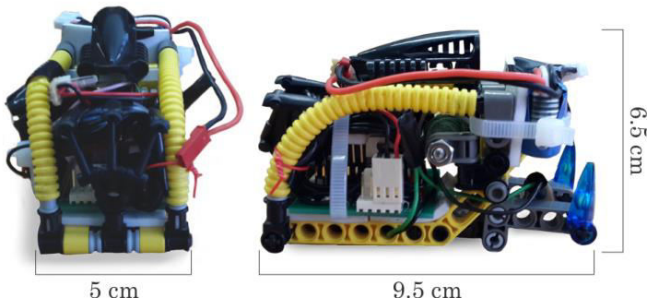

Fig. 10: Front (left) and side (right) views of the LEAP developed for experimentally testing.

As in the simulated tests, the robot's motor would apply a constant resistive force to the line while it was in the air. The duty cycle of the pulse-width-modulated (PWM) signal driving the motor could be varied to control the output force. The accelerometer was used to determine when the robot became airborne: while the robot is supported by the ramp, the accelerometer detects the normal force acting to oppose its weight, therefore by detecting when the magnitude of the force momentarily falls to near-zero, the moment the robot leaves the ramp can be identified and the motor activated.

B. Experimental Design

In total, 24 'silk' jumps – with the dragline attached – and 19 'non-silk' jumps were analysed. Prior to each jump, the robot was left stationary for a period of several hundred samples. The average of the noise over this period was subtracted from the gyroscope readings to remove the sensor bias. The angular velocities would then be rotated from the body frame to the inertial frame using the Euler 2-3-1 sequence[14], and integrated to give the angular position. The equation used to perform the rotation is:

$$\begin{bmatrix}\dot{\phi}_I\\ \dot{\theta}_I\\ \dot{\psi}_I\end{bmatrix} = \begin{bmatrix}1 & -\cos\phi\tan\psi & \sin\phi\tan\psi\\ 0 & \sin\phi & \cos\phi\\ 0 & \cos\phi\sec\psi & -\sin\phi\sec\psi\end{bmatrix}\begin{bmatrix}\dot{\phi}_B\\ \dot{\theta}_B\\ \dot{\psi}_B\end{bmatrix} \quad (7)$$

where $[\dot{\phi}_I \quad \dot{\theta}_I \quad \dot{\psi}_I]^T$ and $[\dot{\phi}_B \quad \dot{\theta}_B \quad \dot{\psi}_B]^T$ are the angular velocity vectors for the inertial and body frames respectively.

By locating the peaks corresponding to the ramp and the collision with the ground on landing, the accelerometer data was used to isolate the period for which the robot was in the air. It was also used to calculate the initial pitch ($\theta_{t=0}$) and roll ($\phi_{t=0}$) in conjunction with the following equations:

$$\theta_{t=0} = \text{asin}(-G_x) \quad (8)$$

$$\phi_{t=0} = \text{asin}\left(\frac{G_y}{\cos\theta_{t=0}}\right) \quad (9)$$

where G_x and G_y are the averages of the accelerations in x and y respectively over the initial stationary period. The initial yaw ($\psi_{t=0}$) was assumed to be zero.

The resolution of the accelerometer equated to 0.4 m s^{-1} per bit, which was not sufficient to accurately determine the linear velocity or position of the robot, so this data was not analysed further. The braking action of the dragline was therefore not investigated experimentally.

IV. Results

A. Experimental Results

In the non-silk jumps, the robot continued to rotate backwards throughout the jump, for a total rotation of (587.0 ± 121.3)° - at least one complete somersault in most cases. In the silk jumps, however, this rotation was reversed and the angular response exhibited the sinusoidal form expected based on the observed spiders and the simulated jumps. Of these jumps, a single pitch reversal occurred in nine jumps while fifteen showed two pitch reversals. This is consistent with the spiders studied, which also typically reversed their pitch twice over a jump with similar relative parameters [7].

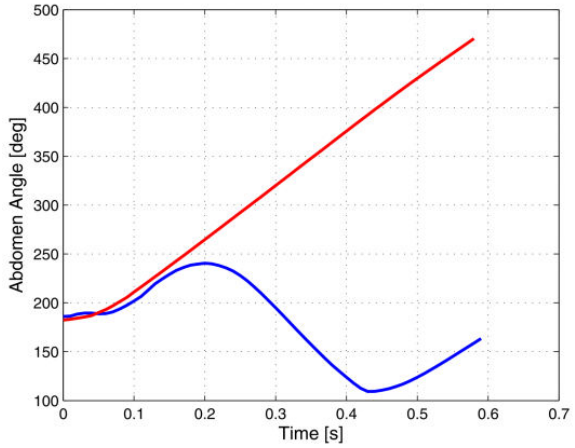

Fig. 11: Plots of θ_A for representative silk (blue) and non-silk (red) jumps made by the LEAP. Without the dragline, it rotates at an approximately constant velocity, while with the dragline the pitch direction is seen to reverse twice.

In the jumps demonstrating a double pitch reversal, the first pitch reversal occurred at an abdomen angle of (244.6 ± 22.3) ° within (149.5 ± 41.0) ms from rest at an initial angle of (188.7 ± 2.6) °. A comparison between the two systems in shown in Fig. 11 and a plot of still images from a representative silk jump is shown in Fig. 12.

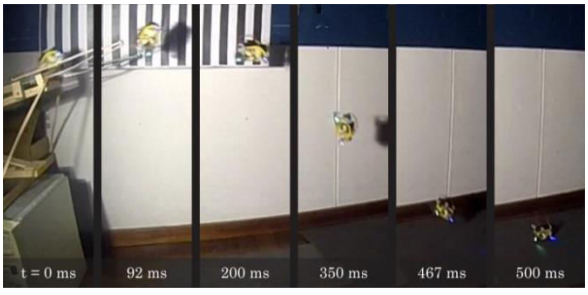

Fig. 12: A plot of representative silk jump where the robot changed its pitch direction twice during the course of the jump.

B. Characteristics of the Dragline Controller

The design of a feedback controller capable of rectifying the pitch using the dragline presents several challenges. Firstly, the system is underactuated [15]: if a particular angle is designated the setpoint, applying tension to the line will either act to increase the error, decrease it or have no effect at all, depending on the instantaneous position of the robot. An effective controller will therefore need to be able to

accurately sense the robot's linear and angular position as well as the silk angle.

In the simulations as well as observations of the spiders in [7], it was noted that the same landing angle can be achieved either by jumping with a lower initial velocity and average silk force, producing a single pitch reversal, or by increasing the force and initial velocity to produce additional reversals. The majority of spiders completed the jump using two pitch reversals [7]. Optimization of the model could be used to determine the optimal motion under different conditions.

The silk jumps studied showed a maximum change in roll angle of (18.2 ± 15.3) ° which was sufficiently small, relative to the pitch changes, for the system to show similar behavior to that predicted by the planar motion model. In jumps with large roll, however, the pitch response was affected erratically, so these were not analysed. This indicates that rotation in other axes does alter the performance of the dragline, and hence the system should also be studied without the restriction of planar motion. By articulating the robot as in [5], the dragline could potentially be adapted to provide angular stabilization in more than one DOF.

The equation derived from the simulations and the presence of the limit cycle indicates that, as long as there is some force on the line, the system will oscillate. For spiders, this means they will always tend to oscillate as they must apply a minimum tension of around 10% of their body weight for the line to be extracted [16]. This is also likely to be the case for mobile robots, as any line-reeling mechanism used will have minimum force required to rotate it.

C. Comparison with Established Righting Methods

Having established that it is indeed possible to correct the pitch of a mobile robot using only a dragline, this mechanism must be evaluated against established aerial righting methods. Compared to angular-momentum-based mechanisms, its first advantage is that it requires only minor additions to the basic robot.

In the observed spiders [7] and in our simulations, the magnitudes of tension required to achieve righting were shown to be small in comparison to the body weight, so if dragline control is implemented using a motor as in the LEAP, a relatively small, low-power device can be selected. In situations where conserving size and weight is important, the cost of a small motor and spool is likely to be far less than the cost of a tail or flywheel.

Although the experimental data was not adequate to confirm these effects in the case of the robot, the simulations showed similar reductions in horizontal velocity to those exhibited in the salticids [7]. Observation of the video footage also showed a general decrease in the range of the silk jumps compared to the non-silk jumps, indicating that the line acted to decrease the linear velocity. This implies that the dragline could have the additional benefit of doubling as a brake to slow the robot to a safe speed before landing.

Besides the potential complexities of implementing a feedback controller utilizing the dragline, its main disadvantage is that it must be connected to the substrate before a jump. This makes it unsuitable for situations involving unplanned ballistic motion or falls.

V. Conclusions and Future Work

This paper has shown that a dragline inspired by salticid jumping spiders has the ability to bring about pitch righting in a mobile robot. It may have additional functionality as a brake, as well as size and weight advantages over more established righting mechanisms, but potential complexities in its feedback control and its unsuitability for use in unexpected falls could make its implementation a challenge.

Future work will examine the effects of the dragline on the linear motion of the robot, as well as its performance in non-planar motion. The results of applying a non-constant force to the line will also be investigated, and the optimal control trajectory determined. Once these areas are better understood, attempts will be made to implement closed loop jump stabilization using the dragline.

Acknowledgements

The authors gratefully acknowledge Prof. Edward Boje and Ms. Robyn Verrinder for their advice and contributions to this research.

References

[1] A. Jusufi, Y. Zeng, R. J. Full, and R. Dudley, "Aerial righting reflexes in flightless animals," *Integr. Comp. Biol.*, vol. 51, no. 6, pp. 937–943, 2011.

[2] J. T. Bingham, J. Lee, R. N. Haksar, J. Ueda, and C. K. Liu, "Orienting in Mid-air through Configuration Changes to Achieve a Rolling Landing for Reducing Impact after a Fall," 2014, no. IEEE International Conference on Intelligent Robots and Systems, pp. 3610–3617.

[3] E. Chang-Siu, T. Libby, M. Tomizuka, and R. J. Full, "A lizard-inspired active tail enables rapid maneuvers and dynamic stabilization in a terrestrial robot," in *IEEE International Conference on Intelligent Robots and Systems*, 2011, pp. 1887–1894.

[4] a Jusufi, D. T. Kawano, T. Libby, and R. J. Full, "Righting and turning in mid-air using appendage inertia: reptile tails, analytical models and bio-inspired robots.," *Bioinspir. Biomim.*, vol. 5, p. 045001, 2010.

[5] E. Chang-Siu, T. Libby, M. Brown, R. J. Full, and M. Tomizuka, "A nonlinear feedback controller for aerial self-righting by a tailed robot," *Proc. - IEEE Int. Conf. Robot. Autom.*, pp. 32–39, 2013.

[6] A. Patel and M. Braae, "Rapid Turning at High - Speed : Inspirations from the Cheetah ' s Tail," in *IEEE International Conference on Intelligent Robots and Systems*, 2013, pp. 5506–5511.

[7] Y.-K. Chen, C.-P. Liao, F.-Y. Tsai, and K.-J. Chi, "More than a safety line: jump-stabilizing silk of salticids.," *J. R. Soc. Interface*, vol. 10, no. 87, p. 20130572, 2013.

[8] F. Vollrath and D. P. Knight, "Structure and function of the silk production pathway in the spider Nephila edulis," *Int. J. Biol. Macromol.*, vol. 24, pp. 243–249, 1999.

[9] D. A. Parry and R. H. J. Brown, "The jumping mechanism of salticid spiders," *J. Exp. Biol.*, vol. 36, pp. 654–466, 1959.

[10] D. E. Hill, "Targeted jumps by salticid spiders (Araneae, Salticidae, Phidippus)," *Version 9*, pp. 1–28, 2006.

[11] T. Weihmann, M. Karner, R. J. Full, and R. Blickhan, "Jumping kinematics in the wandering spider Cupiennius salei," *J. Comp. Physiol. A Neuroethol. Sensory, Neural, Behav. Physiol.*, vol. 196, no. 6, pp. 421–438, 2010.

[12] R. Murray, Z. Li, and S. Sastry, *A Mathematical Introduction to Robotic Manipulation*. CRC Press, 1994.

[13] D. Greenwood, *Advanced Dynamics*. Cambridge: Cambridge University Press, 2003.

[14] J. Diebel, "Representing attitude: Euler angles, unit quaternions, and rotation vectors," *Matrix*, vol. 58, pp. 1–35, 2006.

[15] R. Tedrake, "Fully Actuated vs. Underactuated Systems (Course Notes)," *MIT OpenCourseWear Underactuated Robot.*, 2009.

[16] C. S. Ortlepp and J. M. Gosline, "Consequences of forced silking," *Biomacromolecules*, vol. 5, pp. 727–731, 2004.